NRC·CNRC

NRC Publications Archive
Archives des publications du CNRC

A Continuous Shape Sensitivity Equation Method for Unsteady Laminar Flows

Ilinca, Florin; Pelletier, Daniel

NRC Publications Archive Record / Notice des Archives des publications du CNRC :
https://nrc-publications.canada.ca/eng/view/object/?id=44ca10de-ae09-4dac-bbeb-50caf3d93fbb
https://publications-cnrc.canada.ca/fra/voir/objet/?id=44ca10de-ae09-4dac-bbeb-50caf3d93fbb

Access and use of this website and the material on it are subject to the Terms and Conditions set forth at
https://nrc-publications.canada.ca/eng/copyright
READ THESE TERMS AND CONDITIONS CAREFULLY BEFORE USING THIS WEBSITE.

L'accès à ce site Web et l'utilisation de son contenu sont assujettis aux conditions présentées dans le site
https://publications-cnrc.canada.ca/fra/droits
LISEZ CES CONDITIONS ATTENTIVEMENT AVANT D'UTILISER CE SITE WEB.

Questions? Contact the NRC Publications Archive team at PublicationsArchive-ArchivesPublications@nrc-cnrc.gc.ca. If you wish to email the authors directly, please see the first page of the publication for their contact information.

Vous avez des questions? Nous pouvons vous aider. Pour communiquer directement avec un auteur, consultez la première page de la revue dans laquelle son article a été publié afin de trouver ses coordonnées. Si vous n'arrivez pas à les repérer, communiquez avec nous à PublicationsArchive-ArchivesPublications@nrc-cnrc.gc.ca.

National Research Council Canada | Conseil national de recherches Canada

Canada

imi 2006-113742 - 9
CNRC 48900

European Conference on Computational Fluid Dynamics
ECCOMAS CFD 2006
P. Wesseling, E. Oñate and J. Périaux (Eds)
© TU Delft, The Netherlands, 2006

A CONTINUOUS SHAPE SENSITIVITY EQUATION METHOD FOR UNSTEADY LAMINAR FLOWS

Florin Ilinca* **and Dominique Pelletier†**

*Industrial Materials Institute
National Research Council, Boucherville (Québec), Canada, J4B 6Y4
e-mail: florin.ilinca@cnrc-nrc.gc.ca
†Canada Research Chair, Mechanical Engineering Department
École Polytechnique de Montréal, Montréal (Québec), Canada, H3C 3A7
e-mail: dominique.pelletier@polymtl.ca

Key words: Shape Sensitivity, Flow Control, Finite elements, Unsteady flows

Abstract. *This paper presents the application of a general shape sensitivity equation method to the solution of unsteady laminar flows. The formulation accounts for complex parameter dependence and is suitable for a wide range of problems. The continuous sensitivity equation method (SEM) is first verified on a steady state problem. The computed sensitivity is compared to the actual change in the solution when a small perturbation is imposed to the shape parameter. The methodology is then applied to the flow past a cylinder in ground proximity. The study investigates the ability of the sensitivity equation method to anticipate the unsteady flow response: damping of the vortex shedding when closing the gap to the ground and/or amplification of unsteadiness when the distance to the ground increases.*

1 Introduction

Sensitivity analysis is a relatively new and powerful tool in computational fluid dynamics. A sensitivity (the derivative of the solution with respect to a parameter) indicates how a dependent variable reacts to variations of a design parameter. Sensitivity information finds many uses ranging from driving optimization algorithms, to fast evaluation of nearby flows or to produce uncertainty estimates of the solution. Sensitivities also find applications in flow control due to their ability to indicate the flow response to design parameter changes. In all cases cost-effectiveness is achieved because sensitivities are obtained at a fraction of the cost of computing the flow.

There are several means of computing flow sensitivities: finite differences of flow solutions, the complex step method [1], automatic differentiation [2], and sensitivity equation methods [3, 4, 5]. The first option is costly because the problem must be solved for two or more values of each parameter of interest. Furthermore, technical problems arise because non matching meshes are obtained for different values of a shape parameter. The

complex-step method is code invasive: it requires a complete rewrite of the software in complex variables. While this can be automated, it has a significant impact on performance. Automatic differentiation is equivalent to differentiating the discrete equations to generate a system of equations for the discrete sensitivities. It is powerful because it automatically generates the code for calculating sensitivities. In many cases, implementation requires human intervention to ensure efficiency of the code. Approaches to calculating sensitivities also differ depending on the order of the operations of approximation and differentiation. In the *discrete* sensitivity equation approach, the total derivative of the flow approximation with respect to the parameter is calculated [6], whereas in the *continuous* sensitivity equation method (SEM) one differentiates the continuum equations to yield differential equations for the continuous sensitivities[3]. See Hien et al.[7] for a discussion of the two approaches. We have adopted the latter approach.

Sensitivity analysis is a more advanced field in solid mechanics than in fluid dynamics. Indeed, textbooks have been written on sensitivity analysis of structures [6, 7]. To our knowledge there is only one book on sensitivity analysis of flow problems [4]. It is recent and more specialized than structural mechanics books. Gunzburger [8] discusses sensitivity analysis in the context of flow control and optimization.

Automatic differentiation for first-order flow sensitivities is discussed by Sherman *et al.* [9] and Putko *et al.* [2]. Continuous SEMs may be found in Godfrey and Cliff [10, 11], Borggaard and Burns [3], Limache [12] and Turgeon *et al.* [13] for aerodynamics applications. Application to heat conduction is reported by Blackwell *et al.* [14]. Sensitivities for incompressible flows with heat transfer may be found in several references [5, 15, 16]. Sensitivity analysis for turbulence models is detailed in the works by Godfrey and Cliff [11] and Turgeon *et al.* [17]. Solution of the sensitivity equations for the transient incompressible flow of non-Newtonian fluids is presented by Ilinca and Hétu [18]. A wide variety of flow regimes were treated by the authors [5, 15, 16, 17]. This body of work has shown that sensitivities provide an enriched basis of information on which to develop an understanding of complex flow problems. The work presented here is an extension to unsteady flows of the shape sensitivity methodology presented by Duvigneau and Pelletier [19]. It is also an extension to shape parameters of the unsteady SEM by Hristova *et al.* [20], and Ilinca *et al.* [21] for laminar flows.

The paper is organized as follows. First, we present the equations describing time-dependent laminar flow along with their boundary and initial conditions. The shape sensitivity equations and their boundary/initial conditions are then described in detail. The approach is applied to the flow around a circular cylinder in ground proximity. The methodology and its finite element solver are first verified on a steady state problem. The paper then focuses on unsteady flows and the ability of sensitivities to anticipate important changes in the flow response due to shape changes. We use the example of vortex shedding behind a cylinder in ground proximity. We study to what extent sensitivities can predict amplification/damping of vortex shedding when the ground to cylinder gap varies. The paper ends with conclusions.

2 Flow equations

The flow regime of interest is modeled by the momentum and continuity equations:

$$\rho\frac{\partial \mathbf{u}}{\partial t} + \rho\mathbf{u}\cdot\nabla\mathbf{u} = -\nabla p + \mathbf{f} + \nabla\cdot\left[\mu\left(\nabla\mathbf{u} + (\nabla\mathbf{u})^T\right)\right] \tag{1}$$

$$\nabla\cdot\mathbf{u} = 0 \tag{2}$$

where ρ is the density, $\mathbf{u}$ is the velocity, p is the pressure, μ is the viscosity, t represents time and $\mathbf{f}$ is a body force. The above system is closed with a proper set of initial conditions

$$\mathbf{u}(\mathbf{x}, t=0) = \mathbf{U}_0(\mathbf{x}) \text{ in } \Omega \tag{3}$$

and Dirichlet and Neumann boundary conditions

$$\mathbf{u}(\mathbf{x}, t) = \mathbf{U}_D(\mathbf{x}, t) \text{ on } \Gamma_D \tag{4}$$

$$\mathbf{t} = [-p\mathbf{I} + 2\mu\gamma(\mathbf{u})]\cdot\hat{\mathbf{n}} = \mathbf{F^N} \text{ on } \Gamma_\mathbf{N} \tag{5}$$

where $\mathbf{U}_D$ is the value of the velocity imposed on the boundary Γ_D, $\mathbf{I}$ is the identity tensor, $\gamma(\mathbf{u}) = (\nabla\mathbf{u} + \nabla\mathbf{u^T})/2$ is the shear rate tensor and $\mathbf{F}^N$ is the imposed boundary value of the surface traction force $\mathbf{t}$.

3 Sensitivity Equations

The continuous sensitivity equations (CSE) are derived formally by implicit differentiation of the flow equations (1) and (2) with respect to parameter a. We treat the variable $\mathbf{u}$ as a function of space, time and of the parameter a. This dependence is denoted by $\mathbf{u}(\mathbf{x}, t; a)$. Defining the flow sensitivities as the partial derivatives $\mathbf{s_u} = \frac{\partial \mathbf{u}}{\partial a}$ and $s_p = \frac{\partial p}{\partial a}$, and denoting the derivatives of the fluid properties and other flow parameters by a $(')$, differentiation of equations (1) and (2) yields

$$\rho'\left(\frac{\partial \mathbf{u}}{\partial t} + \mathbf{u}\cdot\nabla\mathbf{u}\right) + \rho\left(\frac{\partial \mathbf{s_u}}{\partial t} + \mathbf{u}\cdot\nabla\mathbf{s_u} + \mathbf{s_u}\cdot\nabla\mathbf{u}\right) = -\nabla s_p + \mathbf{f}'$$
$$+\nabla\cdot\left[\mu'\left(\nabla\mathbf{u} + (\nabla\mathbf{u})^T\right) + \mu\left(\nabla\mathbf{s_u} + (\nabla\mathbf{s_u})^T\right)\right] \tag{6}$$

$$\nabla\cdot\mathbf{s_u} = 0 \tag{7}$$

3.1 Initial and Boundary Conditions

Initial conditions for the sensitivity equations are obtained by implicit differentiation of equation (3)

$$\mathbf{s_u}(\mathbf{x}, t=0) = \frac{\partial \mathbf{U}_0}{\partial a}(\mathbf{x}) \quad \text{in } \Omega, \tag{8}$$

Dirichlet and Neumann boundary condition are obtained in a similar manner. However, if a is a shape parameter, the position of the boundary is also parameter dependent.

Therefore, the differentiation must account for the dependence on a of both the boundary data and the boundary location. The boundary conditions for the CSE are written as:

$$\mathbf{s_u} = \frac{\partial \mathbf{U}_D}{\partial a} - \nabla \mathbf{u} \cdot \frac{\partial \mathbf{x}}{\partial a} \quad \text{on } \Gamma_D \tag{9}$$

$$\begin{aligned}[-s_p \mathbf{I} + 2\left(\mu\gamma(\mathbf{s_u}) + \mu'\gamma(\mathbf{u})\right)] \cdot \hat{\mathbf{n}} = \frac{\partial \mathbf{F}^N}{\partial a} - \left\{\nabla \cdot [-p\mathbf{I} + 2\mu\gamma(\mathbf{u})] \cdot \frac{\partial \mathbf{x}}{\partial a}\right\} \cdot \hat{\mathbf{n}} \\ - [-p\mathbf{I} + 2\mu\gamma(\mathbf{u})] \cdot \frac{\partial \hat{\mathbf{n}}}{\partial a} \quad \text{on } \Gamma_N\end{aligned} \tag{10}$$

As can be seen from equation (9, the flow gradient at the wall are needed to evaluate Dirichlet boundary conditions for the flow sensitivities. Second derivatives of velocity are needed in the case of Neumann boundary conditions. This introduces numerical difficulties when solving CSE, since approximate boundary conditions are used. In this work only the Dirichlet boundary conditions are dependent on the shape parameter. Sensitivity boundary conditions are evaluated by extracting the normal derivatives from the auxiliary fluxes computed on the boundary (see Section 3.3).

3.2 Normal Velocity Boundary Condition

For incompressible flows, the boundary conditions for the velocity sensitivities satisfy strict relationships where Dirichlet boundary conditions are imposed on the flow. Without loss of generality we restrict ourselves to the case of homogeneous Dirichlet conditions. In this specific case, and for shape parameters, the sensitivity of the velocity is always tangent to the surface. This may be a very useful tool for assessing the accuracy of the computed boundary conditions for the sensitivities. To prove that, lets start with the equation (9) for $U_D = 0$:

$$\mathbf{s_u} = -\nabla \mathbf{u} \cdot \frac{\partial \mathbf{x}}{\partial a} \tag{11}$$

which has the scalar components:

$$s_u = -\left[\frac{\partial u}{\partial x}\frac{\partial x}{\partial a} + \frac{\partial u}{\partial y}\frac{\partial y}{\partial a} + \frac{\partial u}{\partial z}\frac{\partial z}{\partial a}\right] \tag{12}$$

$$s_v = -\left[\frac{\partial v}{\partial x}\frac{\partial x}{\partial a} + \frac{\partial v}{\partial y}\frac{\partial y}{\partial a} + \frac{\partial v}{\partial z}\frac{\partial z}{\partial a}\right] \tag{13}$$

$$s_w = -\left[\frac{\partial w}{\partial x}\frac{\partial x}{\partial a} + \frac{\partial w}{\partial y}\frac{\partial y}{\partial a} + \frac{\partial w}{\partial z}\frac{\partial z}{\partial a}\right] \tag{14}$$

The component of the velocity sensitivity normal to the boundary is given by:

$$\begin{aligned}-\mathbf{s_u} \cdot \hat{\mathbf{n}} = \left[\frac{\partial u}{\partial x}n_x + \frac{\partial v}{\partial x}n_y + \frac{\partial w}{\partial x}n_z\right]\frac{\partial x}{\partial a} + \left[\frac{\partial u}{\partial y}n_x + \frac{\partial v}{\partial y}n_y + \frac{\partial w}{\partial y}n_z\right]\frac{\partial y}{\partial a} \\ + \left[\frac{\partial u}{\partial z}n_x + \frac{\partial v}{\partial z}n_y + \frac{\partial w}{\partial z}n_z\right]\frac{\partial z}{\partial a}\end{aligned} \tag{15}$$

where $\hat{\mathbf{n}} = (n_x, n_y, n_z)$ is the direction normal to the boundary and the derivatives of the velocity satisfy the incompressible condition (2):

$$\frac{\partial u}{\partial x} + \frac{\partial v}{\partial y} + \frac{\partial w}{\partial z} = 0 \tag{16}$$

Consider now the first term on the right hand-side of (15) on which we replace $\frac{\partial u}{\partial x}$ by $-(\frac{\partial v}{\partial y} + \frac{\partial w}{\partial z})$, to obtain:

$$\frac{\partial u}{\partial x}n_x + \frac{\partial v}{\partial x}n_y + \frac{\partial w}{\partial x}n_z = \left(\frac{\partial v}{\partial x}n_y - \frac{\partial v}{\partial y}n_x\right) + \left(\frac{\partial w}{\partial x}n_z - \frac{\partial w}{\partial z}n_x\right) \tag{17}$$

Because $\mathbf{u}$ vanishes on the boundary, the derivative of the velocity along any tangent direction $\hat{\mathbf{t}}$ to the boundary is zero: $\nabla\mathbf{u}\cdot\hat{\mathbf{t}} = 0$. Thus, the two terms on the right hand-side of equation (17) vanish, because $(n_y, -n_x, 0)$ and $(n_z, 0, -n_x)$ are two tangent directions and the derivatives of v and w along these directions are zero. A similar treatment applies to the other two terms of equation (15) to obtain:

$$\mathbf{s_u} \cdot \hat{\mathbf{n}} = 0 \tag{18}$$

In the case of a non-homogeneous Dirichlet boundary condition the normal component of the velocity sensitivity is non-zero but it can be determined in terms of the velocity boundary condition. In any case, the normal component is known and can be used as an error estimate to test the accuracy of the computed sensitivity boundary conditions.

3.3 Evaluation of velocity gradient at Dirichlet boundary nodes

For simplicity we restrict ourselves to the case where Dirichlet conditions are specified on the parameter dependent boundary segment. For this case flow gradients at the wall are needed to evaluate boundary conditions via equation (9). To improve accuracy we express the derivatives in the normal and tangential directions as follows

$$\frac{\partial \mathbf{u}}{\partial n} = \frac{\partial \mathbf{u}}{\partial x}n_x + \frac{\partial \mathbf{u}}{\partial y}n_y + \frac{\partial \mathbf{u}}{\partial z}n_z \tag{19}$$

$$\frac{\partial \mathbf{u}}{\partial t_1} = \frac{\partial \mathbf{u}}{\partial x}t_{1x} + \frac{\partial \mathbf{u}}{\partial y}t_{1y} + \frac{\partial \mathbf{u}}{\partial z}t_{1z} \tag{20}$$

$$\frac{\partial \mathbf{u}}{\partial t_2} = \frac{\partial \mathbf{u}}{\partial x}t_{2x} + \frac{\partial \mathbf{u}}{\partial y}t_{2y} + \frac{\partial \mathbf{u}}{\partial z}t_{2z} \tag{21}$$

where $\hat{\mathbf{n}}$ is a unit vector normal to the boundary and $\hat{\mathbf{t}}_1 = (t_{1x}, t_{1y}, t_{1z})$, $\hat{\mathbf{t}}_2 = (t_{2x}, t_{2y}, t_{2z})$ are two orthogonal unit vectors tangent to the boundary. On boundaries with homogeneous Dirichlet condition the tangential derivatives are zero, $\frac{\partial \mathbf{u}}{\partial t_1} = 0$, $\frac{\partial \mathbf{u}}{\partial t_2} = 0$, and we

need only determine the velocity derivative in normal direction. We do this by using the *auxiliary* traction force $\mathbf{t}_b$ [22] on the boundary

$$\int_\Omega \left(\rho\frac{\partial \mathbf{u}}{\partial t} + \rho\mathbf{u}\cdot\nabla\mathbf{u}\right)\mathbf{w}d\Omega - \int_\Omega p\nabla\cdot\mathbf{w} + \int_\Omega \mu\left(\nabla\mathbf{u} + (\nabla\mathbf{u})^T\right) : \nabla\mathbf{w}d\Omega - \int_\Omega f\mathbf{w}d\Omega_P = \int_\Gamma \mathbf{t}_b\mathbf{w}d\Gamma. \quad (22)$$

where

$$\mathbf{t}_b = [-p\mathbf{I} + 2\mu\gamma(\mathbf{u})]\cdot\hat{\mathbf{n}} \quad (23)$$

For incompressible flows and homogeneous Dirichlet conditions equation (23) reduces to

$$\mathbf{t}_b = -p\hat{\mathbf{n}} + \mu\frac{\partial \mathbf{u}}{\partial n} \quad (24)$$

which we use to extract the normal derivative of the velocity at the boundary as

$$\frac{\partial \mathbf{u}}{\partial n} = \frac{1}{\mu}\left(\mathbf{t}_b + p\hat{\mathbf{n}}\right) \quad (25)$$

Finally, cartesian derivatives of the velocity are obtained by solving equations (19), (20) and (21) given the normal and tangential derivatives. Improved accuracy is achieved by projecting the velocity gradient into a divergence free space. This is done by using the incompressibility condition as a constraint when solving equations (19), (20) and (21).

4 Implementation

The flow and sensitivity equations are solved on three-dimensional meshes by a Streamline-Upwind Petrov Galerkin (SUPG) finite element method [23]. Time is discretized by an implicit Euler scheme. The equations are linearized with Newton's method and discretized with the 4-node tetrahedral element using linear interpolants for both velocity and pressure. The same element is used to solve the sensitivity equations. Element matrices are constructed using a numerical Jacobian technique and assembled in a compressed sparse row format. Flow and sensitivity global systems are solved by stabilized BiCG iterative methods.

5 Numerical Results

5.1 Problem statement

We consider the flow around a circular cylinder in ground proximity. The computational domain and boundary conditions are shown on Figure 1. Because the problem is two-dimensional a slab was meshed with one layer of tetrahedral elements. The mesh, shown on Figure 2, was designed to provide adequate flow and sensitivity resolution. The inflow velocity U_0 is uniform. The initial conditions are obtained from a steady state solution of the flow and its sensitivities with respect to s. The Reynolds number $Re = \rho U_0 d/\mu$ is set to 100.

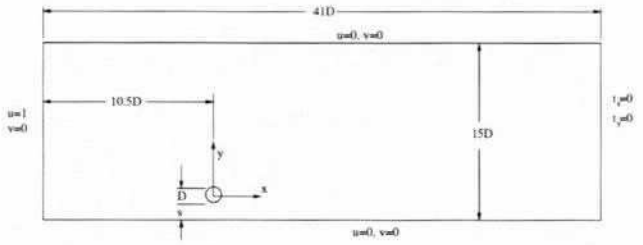

Figure 1: Flow around a circular cylinder in ground proximity: Domain and boundary conditions.

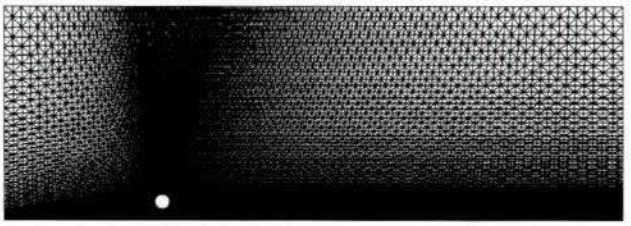

Figure 2: Mesh for the flow around a circular cylinder in ground proximity

5.2 Verification

As shown in section 3, the boundary conditions for the flow sensitivity must be tangent to the cylinder surface. The values of the normal components of the sensitivities are then an indicator of the accuracy of sensitivity boundary conditions. In Figure 3 we show the normal and tangential components of the sensitivity boundary condition. The variable on the x axis represents the angle θ measured counter clockwise from the rear stagnation point on the horizontal axis (ranges from 0 for the point $x = D/2, y = 0$, to $\pi/2$ for $x = 0, y = D/2$, and so on until 2π for $x = D/2, y = 0$). As can be seen, the normal component is very small and it is practically negligible when compared to the tangential component. This indicates that the method used to recover the flow gradients at the wall for evaluating boundary conditions for the sensitivity performs well.

Further verification is done by computing the flow sensitivities with respect to s by finite differences. For this, the distance to the ground s is changed by a small amount δs and the solution is recomputed. In order to minimize the influence of the mesh changes on the solution, the topology of the mesh is kept the same and the only nodes allowed to move are those near the cylinder. The accuracy of the sensitivity is then verified at locations where the mesh does not change with s. The reference finite difference flow sensitivity is determined from

$$\left(\frac{\partial \mathbf{u}}{\partial s}\right)_{FD} = \frac{\mathbf{u}(s+\delta s) - \mathbf{u}(s-\delta s)}{2\delta s} \tag{26}$$

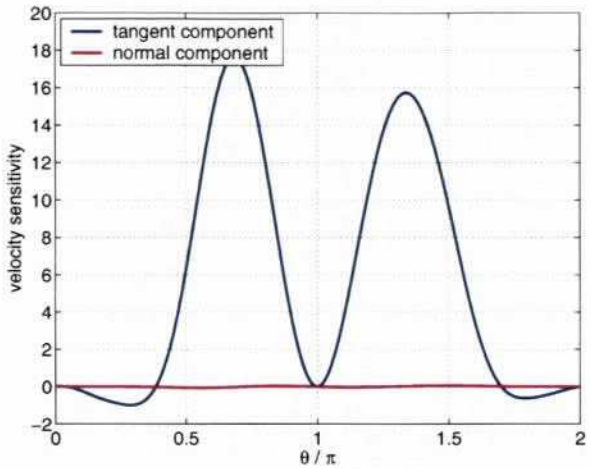

Figure 3: Components of the velocity sensitivity boundary condition on the cylinder surface.

in which δs is taken very small compared to s. In this work we consider $\delta s = 0.001D$. The accuracy of the solution gradient from equation (26) is of the order $\mathcal{O}(\delta s^2)$.

In Figure 4 the sensitivity computed by the proposed CSE method is compared to finite difference approximations (FD) for the steady state solution and $s = 0.75D$. Solutions are compared for the velocity components u and v and for the pressure p at $x = D$, one diameter downstream from the center of the cylinder. As can be seen, the two sets of results agree extremely well indicating that the sensitivity equation method performs well. It also indicates that the flow gradients are computed accurately at the Dirichlet boundary points.

5.3 Sensitivity of the unsteady flow

The flow past the cylinder induces steady-state recirculating vortices for small distances to the wall. When the distance to the wall increases above a critical value, vortex shedding is triggered behind the cylinder resulting in the well known Karman vortex street. We first look at results for the case $s = D$. Figure 5 shows vorticity contours for times $t = 104, 106, 108$, and 110. For this distance to the wall the vortex street develops quite rapidly. To quantify the effect of the wall distance on the vortex street formation, simulations were also carried out for a distance to the wall $s = 0.75D$. Vorticity contours are illustrated in Figure 6 for $t = 118$ to $t = 124$, that is at latter times than for the case $s = D$ (Figure 5). As can be seen, the vortex street develops more slowly and with smaller amplitudes than for the case $s = D$. This is also seen in Figure 7 which compares the time signal of the vertical velocity v at the point $(x = 4D, y = D)$ for the two cases.

Shape sensitivities with respect to the wall distance s were computed for $s = 0.75D$.

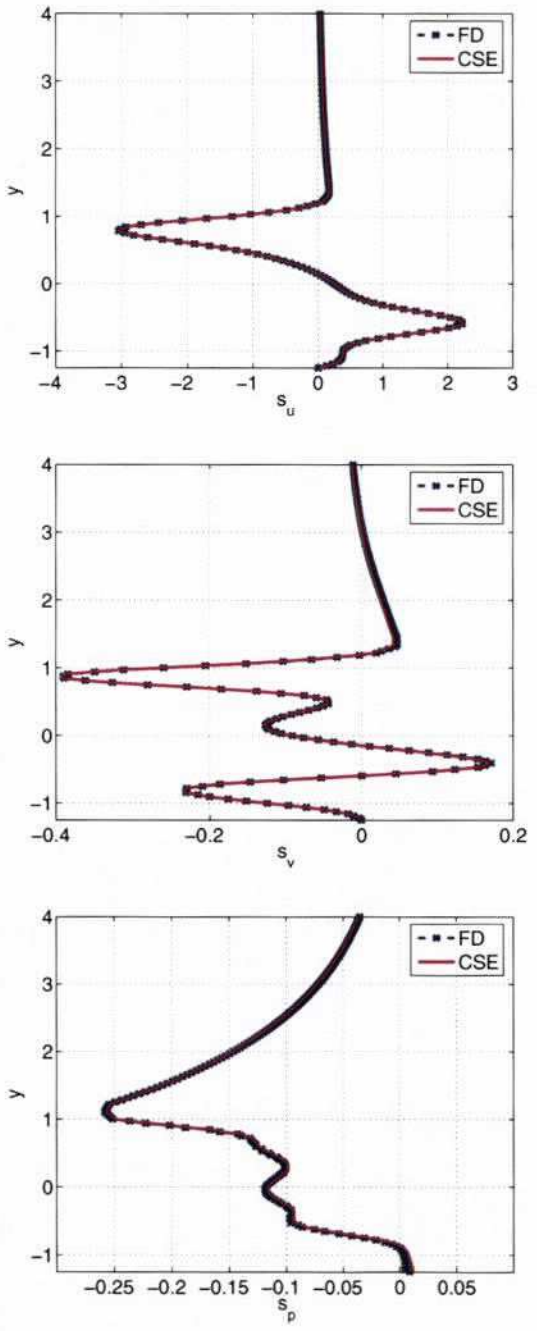

Figure 4: Steady state flow: Verification of the computed sensitivity at $x = D$.

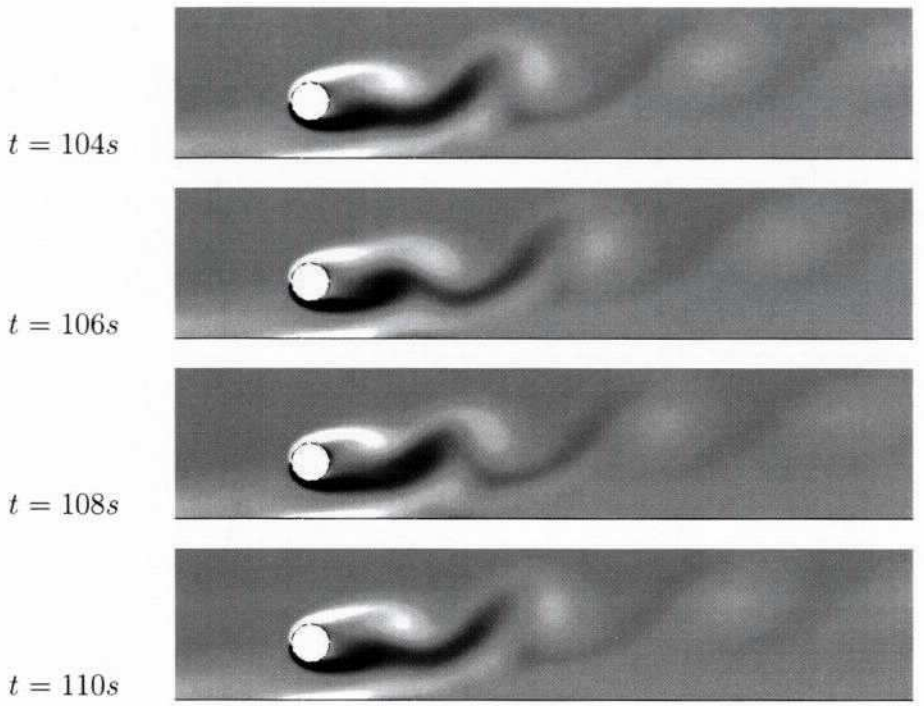

Figure 5: Flow around a circular cylinder at $s = D$ from the wall: Von Karman vortex street.

The time signals at $(x = 4D, y = D)$ for the flow and its sensitivity are shown in Figure 8. The flow solution is shown in the left column of the figure. The SEM sensitivities are compared with a central finite difference approximation with $\delta s = 0.001D$ (FD in Figure 8). The following observations can be made:

- The periods of the sensitivity signals are the same as those of the flow;
- The amplitudes of the oscillation in sensitivities (s_u, s_v, s_p) are larger and increase at a faster rate than those of the flow;
- In all cases the SEM sensitivities agree very well with the finite difference derivatives.

Figure 9 presents the time variations of the oscillation amplitude of the v component of velocity and that of its sensitivity. Both sets of data are plotted on a logarithmic scale because the scale of the velocity oscillations is much smaller that that of its sensitivity. Note that the amplitude of the sensitivity signal is much larger and increases faster than that of the flow solution. This is an important observation because it indicates that the sensitivities appear to be reacting faster than the flow to changes in the parameter values. In other words sensitivities appear able to foretell the transition from the steady-state solution to the vortex shedding before it becomes visible in the flow signal.

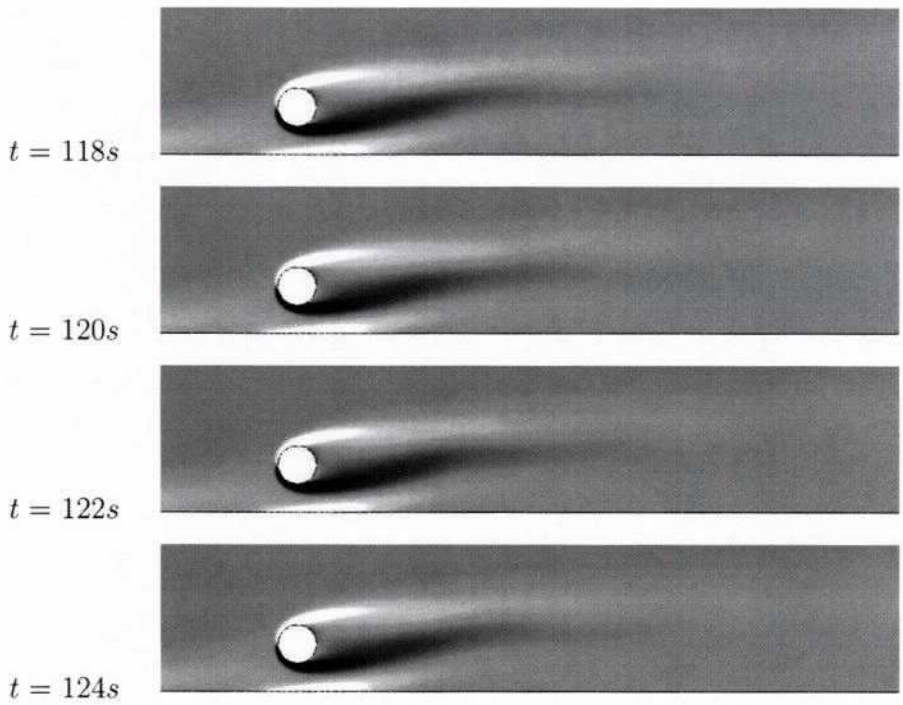

Figure 6: Flow around a circular cylinder at $s = 0.75D$ from the wall: Initiation of unstable flow.

5.4 Fast evaluation of nearby flows

We now show how sensitivities can be used for fast evaluation of nearby flows. Consider for example what happens to the u-velocity, when a generic parameter s is subject to a variation δs from the reference value s_0. The Taylor series expansion give:

$$u(x, y, z, t; s_0 + \delta s) = u(x, y, z, t; s_0) + \left.\frac{\partial u}{\partial s}\right|_{s_0} \delta s + \mathcal{O}(\delta s^2). \tag{27}$$

Using the baseline solution obtained at $s = 0.75D$, we compare the flow estimates from the Taylor series for u and v to a full flow analysis at the perturbed values of the parameter. Results for two values of s, one lower ($s = 0.74D$) and the other larger ($s = 0.76D$) than the baseline value are shown in Figures 10 and 11. The reconstructed solutions are very close to those obtained by reanalysis at the perturbed value of s. The Taylor series approximations of the flow response are in very good agreement with the CFD reanalysis at early times. Agreement deteriorates very slightly at later times, probably because higher order derivatives in the Taylor series expansion become important. Observe also that sensitivities provide useful information above trends of the flow response. They predict the damping of the vortex shedding when s decreases and amplification of unsteadiness when the distance to the ground increases.

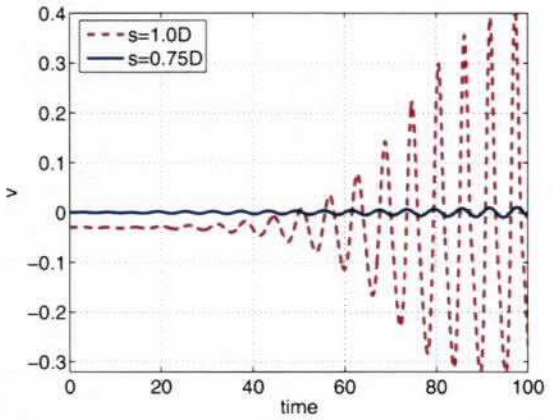

Figure 7: Time signal of the vertical velocity at $(x = 4D, y = D)$.

6 Conclusion

A general shape sensitivity equation formulation was developed for time-dependent incompressible laminar flows. The method is applied to the flow around a circular cylinder in proximity of a solid wall. The study analyzes the influence of the distance to the wall on the transition from the steady-state flow to vortex shedding behind the cylinder. The sensitivity of the flow is computed and correlated with the flow response when the wall distance changes. For $s = 0.75D$, the amplitudes of the sensitivity oscillations increase much faster with time than those of the flow. Hence sensitivities provide useful information to anticipate the flow response. The damping of vortex shedding with decreasing s/D is well predicted. Amplification of shedding with increased s/D is also well predicted. This property of sensitivities will likely prove useful in developing flow control algorithms to maintain certain characteristics of the flow (for example minimize the vortex street or added mass effects).

7 Acknowledgments

This work was sponsored in part by NSERC (Government of Canada), and by the Canada Research Chair Program (Government of Canada).

REFERENCES

[1] J.R.R.A. Martins, P. Stradza, P., and J.J. Alonso. The complex-step derivative approximation. *ACM Trans. Mathem. Software - TOMS*, **29**(3), 245–262, 2003.

[2] M. Putko, P. Newman, A. Taylor, and L. Green. Approach for uncertainty propagation and robust design in CFD using sensitivity derivatives. *15th AIAA Comp. Fluid Dyn. Conf.*, Anaheim, CA, June 2001, AIAA Paper 2001-2528.

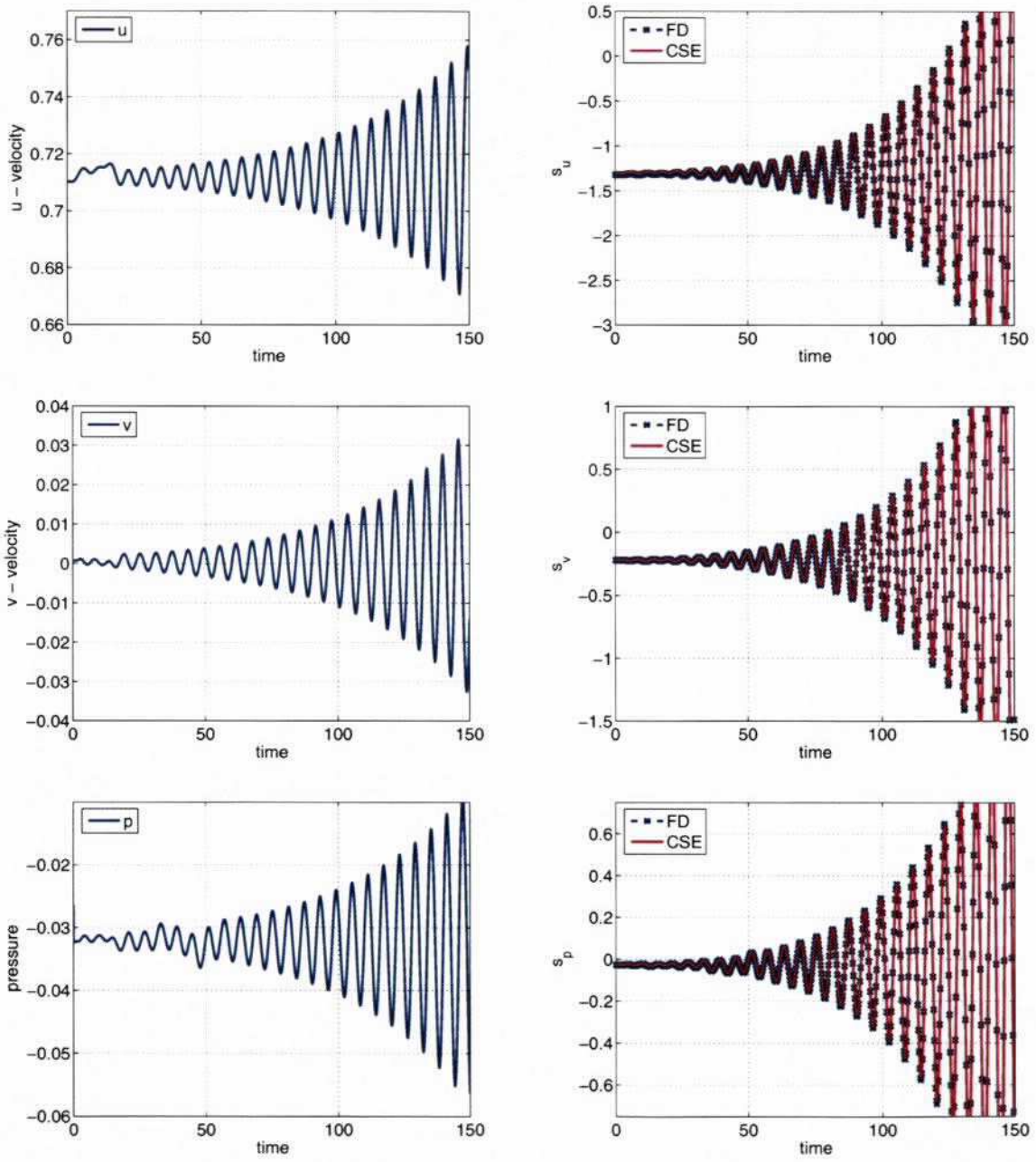

Figure 8: Flow around a circular cylinder: Sensitivities with respect to s at $(x = 4D, y = D)$.

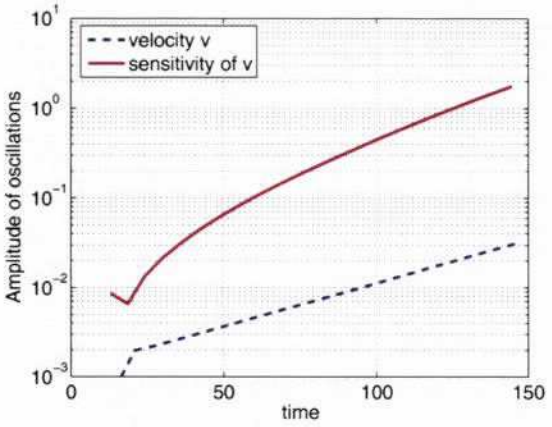

Figure 9: Amplitude of oscillations in v and its sensitivity at $(x = 4D, y = D)$.

[3] J. Borggaard, and J. Burns. A PDE Sensitivity Equation Method for Optimal Aerodynamic Design. *J. of Comp. Physics*, **136**(2), 366–384, 1997.

[4] L.G. Stanley and D.L. Stewart. Design Sensitivity Analysis: Computational Issues of Sensitivity Equation Methods. *Frontiers in Applied Mathematics*, **25**, SIAM, Philadelphia, 2001.

[5] É. Turgeon, D. Pelletier and J. Borggaard. A General Continuous Sensitivity Equation Formulation for Complex Flows. *Num. Heat Transf. B*, **42**, 485–408, 2002.

[6] E.J. Haug, K. Choi and V. Komkov. *Design sensitivity analysis of structural systems*, Vol. 177 of *Mathematics in science and engineering*, Academic Press, Orlando, 1986.

[7] T.D. Hien and M. Kleiber. Stochastic finite element modeling in linear head transfer. *Comp. Meth. Appl. Mech. Eng.*, **144**, 111–124, 1997.

[8] M.D. Gunzburger. *Perspectives in Flow Control and Optimization*, SIAM, 2002.

[9] L.L. Sherman, A.C. Taylor III, L. Green, P.A. Newman, G.W. Hou and V.M. Korivi. First- and second-order aerodynamic sensitivity derivatives via automatic differentiation. *J. Comp. Phys.*, **129**(2), 307–331, 1996.

[10] A.G. Godfrey and E.M. Cliff. Direct Calculation of Aerodynamic Force Derivatives: A Sensitivity-Equation Approach. *36th AIAA Aerospace Science Meeting and Exhibit*, Reno, NV, Jan. 1998, AIAA Paper 98-0393.

[11] A.G. Godfrey and E.M. Cliff. Sensitivity Equations for Turbulent Flows. *39th AIAA Aerospace Sciences Meeting and Exhibit*, Reno, NV, 2001, AIAA Paper 2001-1060.

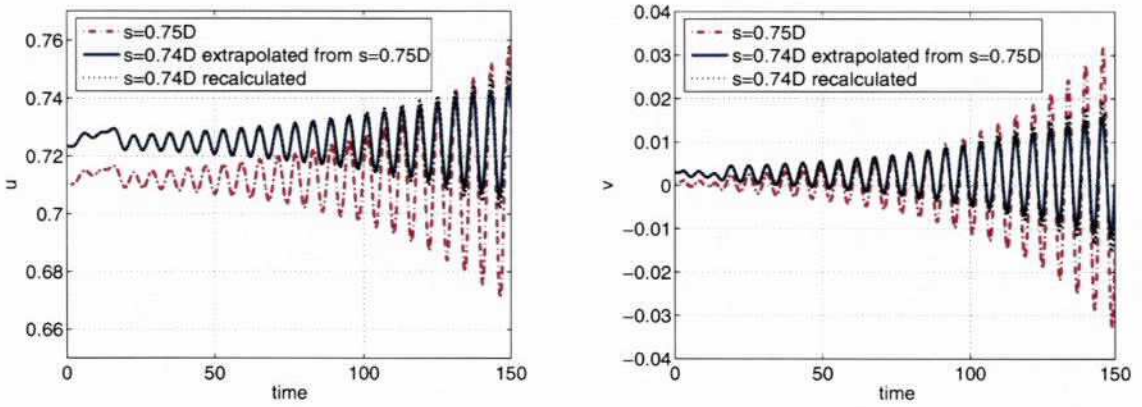

Figure 10: Flow around a circular cylinder: Fast nearby solutions for $s = 0.74D$ at $(x = 4D, y = D)$.

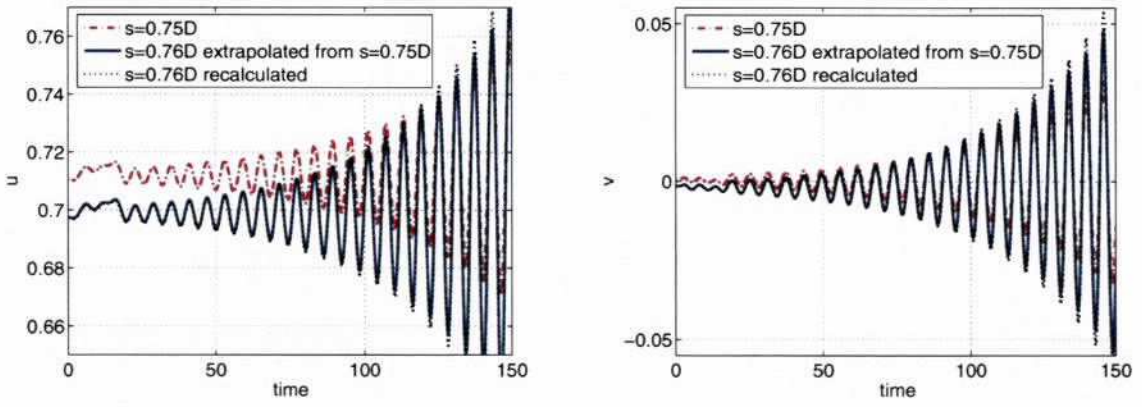

Figure 11: Flow around a circular cylinder: Fast nearby solutions for $s = 0.76D$ at $(x = 4D, y = D)$.

[12] A. Limache. *Aerodynamic Modeling Using Computational Fluid Dynamics and Sensitivity Equations*, Ph.D. thesis, Virginia Polyt. Inst. and State Univ., Blacksburg, VA, 2000.

[13] É. Turgeon, D. Pelletier and J. Borggaard. Computation of Airfoil Flow Derivatives Using a Continuous Sensitivity Equation Method. *8th CASI Aerodynamics Symp.*, Toronto, Canada, April 2001.

[14] B.F. Blackwell, K.J. Dowding, R.J. Cochran and D. Dobranich. Utilization of sensitivity coefficients to guide the design of a Thermal battery. *Proc. 1998 ASME/IMECE*, Anaheim, CA, 1998, pp. 73–82, HTD-Vol. 561-5.

[15] É. Turgeon, J. Borggaard and D. Pelletier. A Continuous Sensitivity Equation Approach to Optimal Design in Mixed Convection. *Num. Heat Trans. A*, **38**, 869–885, 2000.

[16] É. Turgeon, D. Pelletier and J. Borggaard. Application of Continuous Sensitivity Equations to Flows with Temperature-Dependent Properties. *Num. Heat Trans. A*, **44**(6), 611–624, 2003.

[17] É. Turgeon, D. Pelletier and J. Borggaard. A General Continuous Sensitivity Equation Formulation for the $k-\epsilon$ Model of Turbulence. *Int. J. CFD*, **18**, 29–46, 2004.

[18] F. Ilinca and J.-F. Hétu. Three-dimensional Simulation and Design Sensitivity Analysis of the Injection Molding Process. *NUMIFORM 2004*, Columbus, OH, Jun. 2004.

[19] R. Duvigneau and D. Pelletier. Evaluation of Nearby Flows by a Shape Sensitivity Equation Method. *43th AIAA Aerospace Sciences Meeting and Exhibit*, Reno, NV, Jan. 2005, AIAA-2005-0127.

[20] H. Hristova, S. Étienne, D. Pelletier and J. Borggaard. A Continuous Sensitivity Equation Method for Time-Dependent Incompressible Laminar Flows. *Int. J. Num. Meth. Fluids*, **50**, 817–844, 2005.

[21] F. Ilinca, D. Pelletier and J. Borggaard. A Continuous Second Order Sensitivity Equation Method for Time-Dependent Incompressible Laminar Flows. *17th AIAA Computational Fluid Dynamics Conference*, Toronto, ON, 2005, AIAA-2005-5100.

[22] T.J.R. Hughes, G. Engel, L. Mazzei and M.G. Larson. The continuous Galerkin method is locally conservative. *J. of Comp. Phys.*, **163**, 467–488, 2000.

[23] F. Ilinca, J.-F. Hétu and D. Pelletier. On stabilized finite element formulations for incompressible advective-diffusive transport and fluid flow problems. *Comp. Meth. Appl. Mech. Eng.*, **188**(1-3), 235–255, 2000.